

# Optoelectronic Oscillators for High Speed and High Resolution Optical Sensing

Jianping Yao, *Fellow, IEEE, Fellow, OSA*

(Invited Paper)

**Abstract**—An optoelectronic oscillator (OEO) can be employed to perform high speed and ultra-high resolution optical sensing. The fundamental concept is to convert a measurand-dependent wavelength change in the optical domain to a frequency change of an OEO-generated microwave signal in the microwave domain. Since the frequency of a microwave signal can be measured by a digital signal processor at a high speed and high resolution, an OEO-based optical sensor is able to provide optical interrogation at a high speed and ultra-high resolution. In this paper, OEO-based optical sensors proposed for strain, temperature, or transverse load sensing are discussed. The key to implement an OEO-based optical sensor is to implement a microwave photonic filter with a passband having a center frequency that is a function of the optical wavelength change. In this paper, techniques to implement microwave photonic filter for OEO-based optical sensing are discussed.

**Index Terms**—Fiber Bragg grating, microwave photonics, optical sensor, optoelectronic oscillator.

## I. INTRODUCTION

THE concept of optoelectronic oscillators (OEO) was originally proposed in early 80s [1] which was further studied with an objective of generating a high-frequency and low-phase-noise microwave signal which may not be generated by electronic oscillators or electronic frequency synthesizers [2]. An OEO has a hybrid feedback loop consisting of an electrical path and an optical path. Since the loss of an optical fiber is very small, the optical path can be implemented using a long optical fiber. A longer OEO loop corresponds to a higher Q factor. An OEO with a high Q factor is important for the generation of a high-quality microwave signal with low phase noise. On the other hand, an OEO can also be used as a high speed and high resolution optical sensor [3]. The fundamental concept of using an OEO for optical sensing is to convert the optical wavelength change caused by a strain, transverse load, temperature or refractive index change to a frequency change in an OEO-generated microwave signal. Since the frequency of a microwave signal can be measured

using a high speed digital signal processor (DSP), the interrogation speed and resolution can be much higher than using an optical spectrum analyzer (OSA) which is widely used for interrogation in a conventional optical sensor system. In the last few years, numerous efforts have been directed to the design and implementation of new OEO architectures for strain, temperature or transverse load sensing and numerous solutions have been proposed. In the paper, an overview of OEO-based optical sensors with high interrogation speed and high resolution is presented. The key device in an OEO-based optical sensor is a microwave photonic filter, which should have a passband with a center frequency that is a function of the optical wavelength change. In this paper, four different OEO architectures using four different microwave photonic filters for OEO-based optical sensing are discussed.

In the first architecture, an OEO with its oscillation frequency determined by a microwave photonic filter to conduct extremely fast fiber Bragg grating (FBG) strain sensing is discussed [4]. The key device in the OEO is the microwave photonic filter which is employed as an oscillation frequency selection element as well as a sensing element. The microwave photonic filter is realized using a laser diode (LD), a phase modulator (PM), a phase-shifted fiber Bragg grating (PS-FBG), and a photodetector (PD). By converting a phase-modulated signal to a single-sideband intensity-modulated signal using the PS-FBG to filter out one of the two first-order sidebands of a phase-modulated signal, a microwave bandpass filter with its center frequency determined by the wavelength difference between the wavelength of the optical carrier and the central wavelength of the notch of the PS-FBG is implemented [5]. If a strain is applied to the PS-FBG, the notch wavelength would be shifted, which is translated to a microwave frequency change. By measuring the microwave frequency change, the strain applied to the PS-FBG is measured.

In the second architecture, an OEO incorporating a dual passband microwave photonic filter for temperature-insensitive transverse load sensing is discussed. The dual passband microwave photonic filter is implemented using an LD, a PM and polarization-maintaining PS-FBG (PM-PS-FBG) [6]. The dual passbands are produced due to the birefringence of the PM-PS-FBG which has two notches along the two principal axes. By incorporating the dual-bandpass microwave photonic filter into the OEO, two oscillation frequencies would be generated. Due to the nonlinearity of the PM a third frequency which

Manuscript received May 31, 2016; accepted June 23, 2016. Date of publication June 28, 2016; date of current version June 24, 2017. This work was supported by the Natural Sciences and Engineering Research Council of Canada.

The author is with Microwave Photonics Research Laboratory, School of Electrical Engineering and Computer Science, University of Ottawa, Ottawa, ON K1N 6N5, Canada (e-mail: jpyao@eecs.uottawa.ca).

Color versions of one or more of the figures in this paper are available online at <http://ieeexplore.ieee.org>.

Digital Object Identifier 10.1109/JLT.2016.2586181

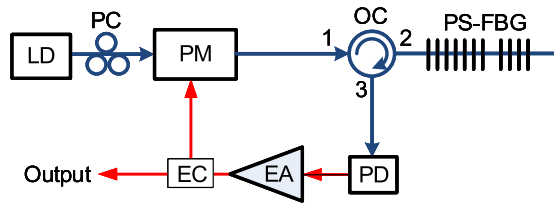


Fig. 1. Schematic of an OEO sensor based on a PS-FBG. LD: laser diode, PC: polarization controller; PM: phase modulator, OC: optical circulator, PS-FBG: phase-shifted fiber Bragg grating, PD: photodetector, EA: electrical amplifier, EC: electrical coupler.

is the beat note between the two generated microwave signals would be generated. Since the two microwave frequencies are experiencing the same frequency shift due to the same temperature change, the third frequency is temperature insensitive. By measuring the frequency change of the third frequency, a temperature-insensitive transverse load sensor is implemented.

In the third architecture, the LD in the OEO is replaced by a broadband light source. The advantage of using a broadband light source is that the frequency drift existing in a laser source which would cause interrogation errors does not exist [7]. Again, the oscillation frequency of the OEO is determined by a microwave photonic filter, which is implemented using the broadband light source, a Mach-Zehnder interferometer (MZI), a dispersion compensating fiber (DCF), and a PD. One arm of the MZI is used as a sensing arm which is exposed to a strain or temperature and the other arm is used as a reference arm. When the strain or temperature is changed, the length difference between the two arms is changed, which leads to the change in the free spectral range (FSR) of the MZI. Since the central frequency of the microwave photonic filter is a function of the FSR, the oscillation frequency of the OEO is affected by the strain or temperature applied to the sensing arm. By measuring the frequency change, the temperature change to the sensing arm can be measured.

In the fourth architecture, a high-resolution transverse load fiber-optic sensor based on an OEO-coupled dual-wavelength fiber ring laser with improved lasing stability is discussed [8]. The use of an OEO-coupled dual-wavelength laser source instead of an independent laser source can eliminate the wavelength-drift-induced interrogation errors. The fiber-optic sensor has two mutually coupled loops, the fiber ring loop and the OEO loop. A PM-PS-FBG is incorporated in the fiber ring loop to generate two optical wavelengths with the wavelength spacing determined by the wavelength difference between the two notches of the PM-PS-FBG along the two principal axes of the PM fiber. In the OEO loop, a microwave signal with its frequency also determined by the wavelength difference between the two notches is generated, which is fed into the fiber ring loop to injection lock the dual wavelengths to ensure a very stable dual-wavelength operation. Since the wavelength spacing is determined by the birefringence, wavelength drifts will not affect the generated microwave frequency, ensuring a wavelength-drift-independent interrogation. The use of the OEO sensor for high-speed and high-resolution transverse load sensing is implemented.

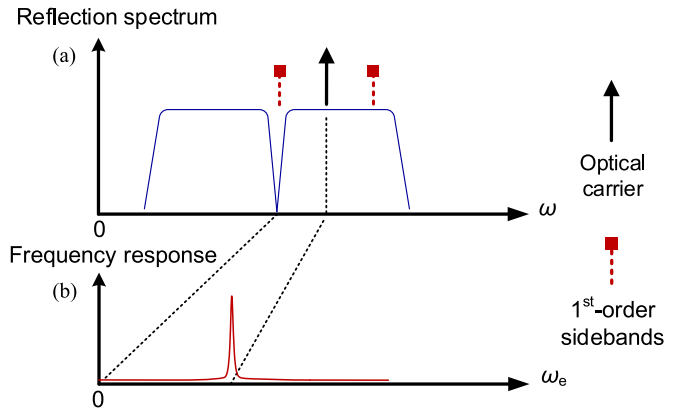


Fig. 2. The operation of an OEO sensor based on a PS-FBG. (a) The reflection spectrum of the PS-FBG, and (b) the frequency response of the microwave photonic filter.

## II. A STRAIN SENSOR BASED ON AN OEO

A high-speed and high-resolution strain sensor can be implemented using an OEO [4]. In general, an OEO has a hybrid loop consisting of two paths, an optical path and an electrical path. Fig. 1 shows the schematic of an OEO. As can be seen the OEO consists of an LD, a PM, a PS-FBG, a PD and an electrical amplifier (EA). When the loop is closed, a phase-modulated optical signal is generated, which is sent to the PS-FBG. The PS-FBG has a transmission spectrum with an ultra-narrow notch, as shown in Fig. 2(a). One sideband of the phase modulated signal is removed by the PS-FBG, and a single-sideband with carrier signal is obtained at the output of the PS-FBG. The beating between the optical carrier and the remaining sideband will generate a microwave signal which is amplified by the EA and sent back to the PM. If the gain provided by the EA is sufficiently large to compensate for the loss of the loop, oscillation will start. The oscillation frequency is determined by the wavelength spacing between the optical carrier and the notch of the PS-FBG.

The key device in the OEO is the microwave photonic filter which is employed as an oscillation frequency selection element as well as a sensing element. Fig. 2(a) and (b) shows the operation of a microwave photonic filter. As can be seen a phase-modulated signal is generated at the PM and is sent to the PS-FBG. We know that a phase-modulated signal has two first-order sidebands with an optical carrier. The difference between a phase-modulated optical signal and an intensity-modulated optical signal is that the two first-order sidebands are in phase for an intensity-modulated, but out of phase for a phase-modulated optical signal. If a phase-modulated signal is sent to a PD directly, no microwave signal will be detected since the beating between the optical carrier and the upper first-order sideband will cancel completely the beating between the optical carrier and the lower first-order sideband. However, if one of the first order sidebands is eliminated by the notch of the PS-FBG, a microwave signal that is the beating between the optical carrier and the remaining sideband will be generated. The overall operation is equivalent to a microwave photonic filter with the center frequency equal to the frequency difference

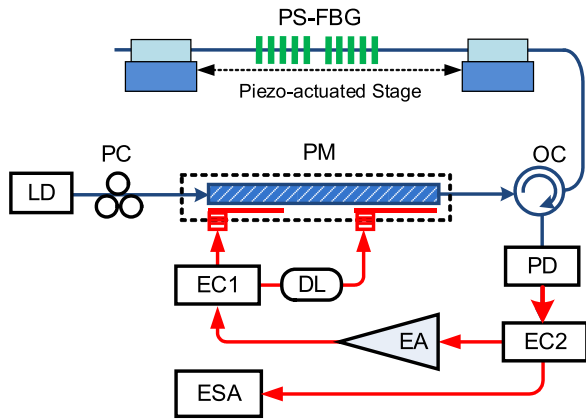


Fig. 3. Experimental setup for the evaluation of the OEO for strain sensing [4]. LD: laser diode; PC: polarization controller; PM: phase modulator; OC: optical circulator; PD: photodetector; EC: electrical coupler; EA: electrical amplifier; DL: delay line; ESA: electrical spectrum analyzer.

between the optical carrier and the notch. When the loop is closed and the gain of the EA is sufficiently large to compensate for the loss of the loop, oscillation will start and a microwave signal will be generated.

When a strain is applied to the PS-FBG, the center wavelength of the spectrum of the PS-FBG will shift due to the variation of the grating pitch, thus the spacing between the optical carrier and the notch will be changed, which would lead to a change to the center frequency of the microwave photonic filter, and thus the frequency of the generated microwave signal. By measuring the microwave frequency change, the strain can be measured. The use of an OEO as an optical sensor is to translate the optical domain measurement into an electrical spectrum measurement, thus ensuring a significantly higher frequency resolution. The wavelength resolution is ultimately limited by the frequency spacing of the oscillating modes in the OEO. In addition, the microwave signal generated by an OEO has a much higher signal-to-noise ratio (SNR) than a signal obtained through wavelength-to-intensity conversion using an edge filter [9], [10], thus the use of an oscillation scheme has also a very positive impact on the measurement SNR performance.

Fig. 3 shows an experimental setup for the evaluation of the OEO for strain sensing. A two-port PM is used. A microwave signal is sent to the PM through the two ports with a time delay introduced by an electrical delay line. This is equivalent to a two-tap microwave filter. The motivation of using the two-tap microwave filter is to further reduce the bandwidth of the microwave photonic filter to ensure a single frequency operation of the OEO. The phase-modulated light wave is sent to the PS-FBG through the optical circulator (OC) and the reflected signal is sent to the PD to generate a microwave signal. After electrical amplification by the EA, the microwave signal is split into two paths by two electrical couplers (EC1 and EC2). One is applied to the PM to close the OEO loop. The other is sent to an electrical spectrum analyzer (ESA). The open-loop response of the OEO corresponds to a microwave bandpass filter with a bandwidth of only a few tens of MHz.

The PS-FBG was fabricated by introducing a phase shift during the FBG fabrication process and was mounted on a piezo-actuated stage. The central wavelength of the transmission

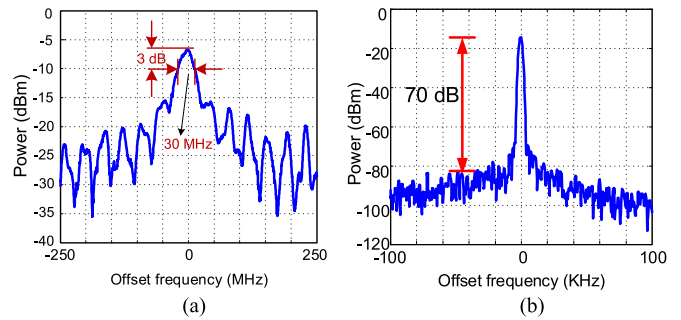


Fig. 4. (a) Measured frequency response of the microwave photonic filter. (b) Spectrum of a 10-GHz microwave signal generated by the OEO [4].

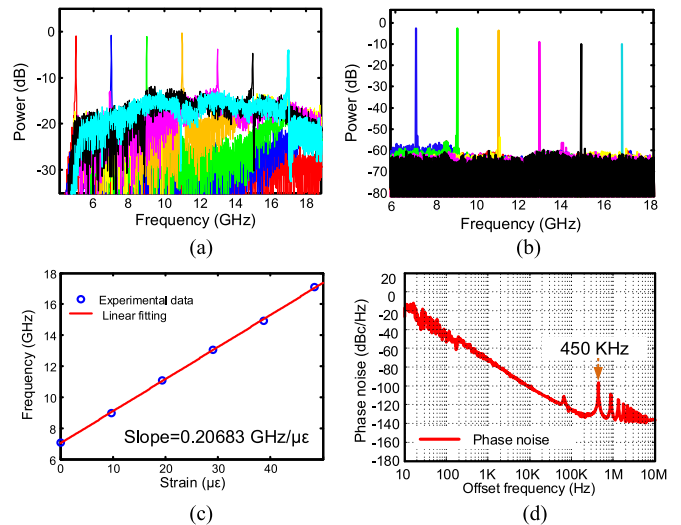


Fig. 5. (a) Measured frequency response of the microwave filter for different applied strains. (b) Spectra of the generated microwave signal for different strains. (c) Relationship between the applied strain and the frequency of the generated microwave signal. (d) The phase noise measurement of the generated microwave signal at 10 GHz [4].

band is about 1549.28 nm, with a full-width at half-maximum width of only about 30 MHz, which determines the bandwidth of the microwave filter of the open loop OEO, as shown in Fig. 4(a). When the OEO loop is closed, a microwave signal with a frequency at 10 GHz and a 70-dB sidemode suppression ratio is generated, as shown in Fig. 4(b). The 70-dB sidemode suppression ratio is related to the SNR of the wavelength interrogation scheme, well beyond the achievable values by any other techniques. When the resonance wavelength of the PS-FBG is shifted, due to a strain change, for example, the frequency of the generated microwave signal is then accordingly shifted and can be easily measured using a DSP. Fig. 5(a) shows the measured frequency response of the microwave filter for different axial strains applied to the PS-FBG. The spectra of the generated microwave signals corresponding to the different applied strains are shown in Fig. 5(b). The frequency of the generated microwave signal is shifted from about 7 to 17 GHz. The measurements confirm the expected linear relationship between the applied strain and the frequency of the generated microwave signal, as shown in Fig. 5(c). The phase noise of a generated microwave signal at 10 GHz is also measured, which is shown in Fig. 5(d). As can be seen, a phase noise of  $-100$  dBc/Hz at an offset of 10 kHz is achieved. Several peaks are observed

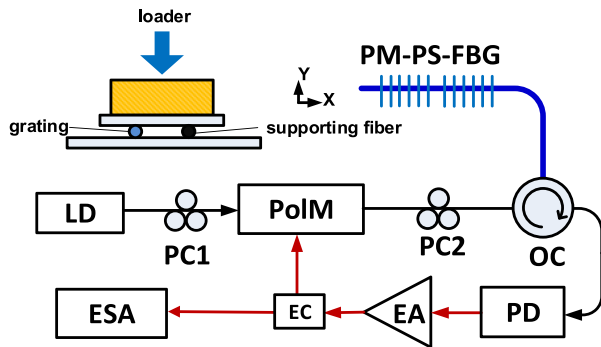


Fig. 6. A temperature-insensitive transverse load sensor based on a dual-frequency OEO [6]. LD: laser diode; PolM: polarization modulator; PC: polarization controller; PD: photodetector; EA: electrical amplifier; ESA: electrical spectrum analyzer.

for offset frequencies equal or greater than 450 KHz. This frequency (450 KHz) corresponds to the longitudinal mode spacing of the OEO. When the resonance wavelength of the PS-FBG is shifted due to a strain applied to the PS-FBG with a frequency (wavelength) shift  $>450$  kHz or equivalently  $>360$  fm, the frequency of the generated microwave signal is then accordingly shifted. Thus, the longitudinal mode spacing defines the resolution of the OEO as an optical sensor. To increase the resolution, the loop length should be increased, but a microwave filter with a narrow bandwidth should be used to ensure a single frequency operation.

### III. A TEMPERATURE-INSENSITIVE TRANSVERSE LOAD SENSOR BASED ON A DUAL-FREQUENCY OEO

The key to achieve an OEO-based optical sensor is to implement a microwave photonic filter with its center frequency being a function of the optical wavelength change. Thus, when a measurand is changed, the wavelength is changed and the center frequency is changed, which leads to the change of the generated microwave signal. For the OEO-based sensor shown in Fig. 1, the change in strain or temperature will both lead to a change in wavelength. Thus, it is not possible to separate the strain and temperature measurement. A solution is to use a PM-PS-FBG to replace the single-mode PS-FBG in Fig. 3 [6]. Due to the birefringence of the fiber in which a PM-PS-FBG is inscribed, two reflection bands that have slightly different center frequencies along the two principal axes of the fiber are resulted. If the PM-PS-FBG is jointly used with an LD, a polarization modulator (PolM) and a PD, a dual passband microwave filter will be implemented. By incorporating the dual passband microwave filter into an OEO, a dual frequency OEO will be realized. Note that the PolM is a special PM that supports phase modulation along the orthogonal principal axes with complementary phase modulation indices. When a temperature change is applied to the PM-PS-FBG, the center frequencies of the two passbands will experience the same frequency shift, and the difference between the two wavelengths is maintained unchanged. By incorporating the PM-PS-FBG into an OEO, a dual frequency oscillation can be generated and the beating between the two frequencies will generate a third frequency which is temperature insensitive. Fig. 6 shows the PM-PS-FBG

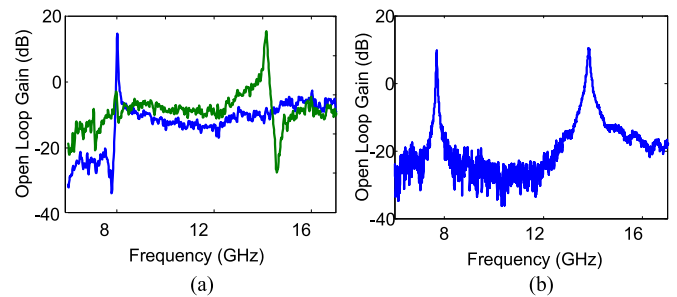


Fig. 7. (a) The spectrums of a single passband photonic microwave filter when the polarization of the incident light wave is aligned with an angle of  $0^\circ$  or  $90^\circ$  relative to one principal axis of the PolM. (b) The spectrum of a dual passband photonic microwave filter when the polarization of the incident light wave is aligned with an angle of  $45^\circ$  relative to one principal axis of the PolM [6].

based OEO sensor configuration. A light wave generated by an LD is sent to a PolM via a PC (PC1). If the polarization direction of the incident light wave is aligned with one of the principal axes, the PolM is operating as a regular PM. The phase-modulated signal is then sent to the PM-PS-FBG through an OC. One sideband of the phase-modulated signal is filtered out by the notch of the PM-PS-FBG, and the phase-modulated signal is converted to a single-sideband intensity-modulated signal and is detected at a PD. The detected electrical signal is sent back to the PolM after amplification by an EA, to close the OEO loop. The entire operation is equivalent to a microwave photonic filter, with the central frequency of the passband determined by the wavelength spacing between the optical carrier and the notch.

Fig. 7(a) shows the passband of the microwave photonic filter along the horizontal or vertical polarization direction, measured by aligning the polarization of the incident light wave having an angle of  $0^\circ$  or  $90^\circ$  relative to one principal axis of the PolM. When the polarization of the incident light wave is aligned with an angle of  $45^\circ$  relative to one principal axis of the PolM, the light wave is equally projected to the two orthogonal polarization axes, thus a photonic microwave filter with two passbands is implemented. Fig. 7(b) shows the frequency response when the polarization of the incident light wave is aligned with an angle of  $45^\circ$  relative to one principal axis of the PolM. A dual passband filter is realized. When the OEO loop is closed, two microwave signals at two frequencies determined by the two passbands are generated. If a transverse load is applied to the PM-PS-FBG, the central frequencies of the two passbands will be shifted and the corresponding oscillation frequencies of the microwave signals will also be shifted. Due to the nonlinearity of the PolM, a third frequency corresponding to the beat signal between the two microwave signals is also generated, as shown in Fig. 8. Since the two oscillation frequencies experience an identical frequency shift due to temperature change, the frequency of the beat note is only associated with the birefringence introduced by the transverse load to the PS-FBG. Thus, by measuring the beat frequency, the transverse load is measured.

If a transverse load is applied to the PM-PS-FBG, a change in the beat frequency corresponding to the applied transverse load is generated. For real implementation, the transverse load should be applied to the PM-PS-FBG along the fast or slow axis to ensure the sensor to reach its highest sensitivity and to

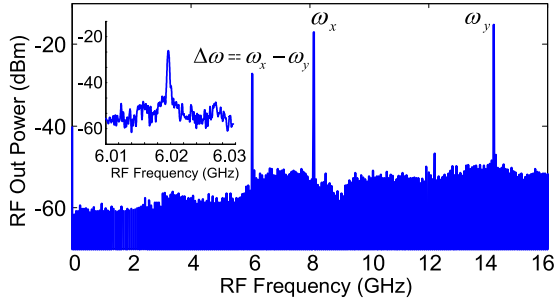


Fig. 8. The electrical spectrum of the signal generated by the dual-frequency OEO. Two microwave signals at 8.22 GHz and 14.24 GHz are generated by the OEO, and a beat signal at 6.02 GHz is also generated. The inset gives a zoom-in view of the spectrum of the beat signal [6].

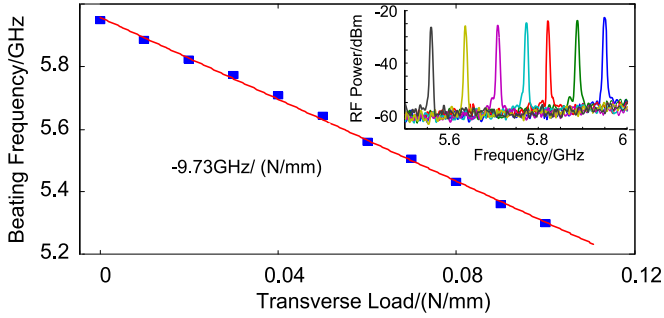


Fig. 9. Measured beat frequency as a function of the transverse load. The inset shows the electrical spectrums with different transverse loads [6].

have a good linearity between the transverse load and the beat frequency. In the experiment, a supporting fiber with an identical radius was placed in parallel with the PS-FBG to make the load be applied to the PM-PS-FBG transversely, while sharing half of the applied load. By applying the load along the fast axis and increasing the load applied to the PS-FBG, the beat frequency is shifted linearly towards a smaller frequency, as shown in Fig. 9. The spectrum of the beat signal is measured by an ESA, with the spectrum shown in the inset of Fig. 9. The relationship between the transverse load the beat frequency is given by  $d\nu/dF \approx 9.9 \text{ GHz}/(\text{N}/\text{mm})$  which is obtained by using the typical values of a silica fiber. Through linear fitting the slope is  $-9.73 \text{ GHz}/(\text{N}/\text{mm})$  which agrees well with the theoretical value of  $9.9 \text{ GHz}/(\text{N}/\text{mm})$ .

#### IV. AN OEO SENSOR USING A BROADBAND LIGHT SOURCE

The OEO-based sensors discussed in Sections II and III are implemented using an LD as a light source. The frequency of the generated microwave signal is determined by the wavelength difference between the optical carrier and the notch of the PS-FBG or notches of the PM-PS-FBG. If the wavelength of the optical carrier is changed, an interrogation error will be resulted. A solution to this problem is to use a broadband light source [7]. Fig. 10 shows the schematic of an OEO using a broadband light source. As can be seen the light wave from a broadband amplified spontaneous emission (ASE) source is coupled into an MZI with two unequal-length arms with a length difference of  $\Delta L$ . The upper arm is used as a sensing arm and the lower arm

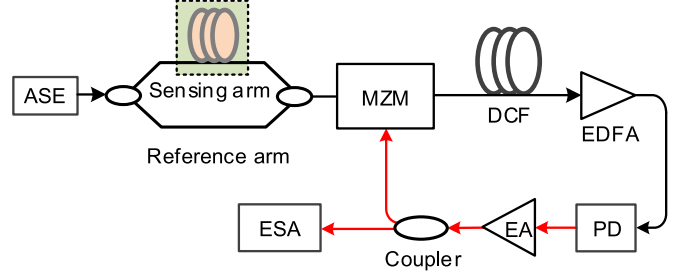


Fig. 10. Schematic of an OEO sensor based on a broadband light source [7]. ASE: amplified spontaneous emission. MZM: Mach-Zehnder modulator. DCF: dispersion compensating fiber. EDFA: erbium-doped fiber amplifier. PD: photodetector. EA: electrical amplifier. ESA: electrical spectrum analyzer.

as a reference arm. When a strain or temperature applied to the sensing arm is changed, the length difference between the two arms is changed, which would lead to the change in the FSR of the MZI. Note that the spectra response of the MZI has a shape that is sinusoidal. The broadband light from the ASE source is sliced by the MZI, which lead to an amplitude tailored light wave with a sinusoidal envelope. The spectrum-sliced broadband light wave is then coupled into an MZM biased at the quadrature point. The modulated light wave is sent to a length of a DCF serving as a dispersive element. After amplification by an erbium-doped fiber amplifier (EDFA), the light wave is sent to a PD. The electrical signal at the output of the PD is amplified by an EA and fed back to the MZM to form the OEO loop.

The key to achieve single-frequency oscillation is to have a microwave photonic filter with a narrow passband. This is done by a joint use of a sinusoidal-shaped broadband light wave, an MZM, a DCF and a PD. The operation corresponds to a single bandpass microwave photonic filter with its bandpass frequency determined by the FSR of the MZI, the dispersion of the DCF [11], [12], given by

$$f_0 = \frac{1}{D\Delta\lambda_{\text{FSR}}^0} = \frac{n_{\text{eff}}\Delta L_0}{D\lambda^2} \quad (1)$$

where  $D$  is the value of the group velocity dispersion (ps/nm) of the DCF,  $\Delta\lambda_{\text{FSR}}^0$  is the original FSR of the MZI without the influence of a strain or temperature change which is expressed as  $\Delta\lambda_{\text{FSR}}^0 = \lambda^2/(n_{\text{eff}}\Delta L_0)$ , where  $\lambda$  is the wavelength of the incident light wave,  $n_{\text{eff}}$  is the effective refractive index of the fiber core, and  $\Delta L_0$  is the original length difference between the two arms without experiencing a strain or temperature change.

When the microwave photonic filter is incorporated in the OEO, a microwave signal with a frequency equal to the center frequency of the microwave photonic filter is generated. For a given total dispersion of the OEO loop, the frequency of the microwave signal is uniquely determined by the FSR of the MZI, which is linearly proportional to the length difference between the two arms of the MZI. Therefore, when a strain or temperature applied to the sensing arm is changed, the length difference between the two arms of the MZI is changed, and the FSR is also changed, which would lead to a change in the generated microwave frequency.

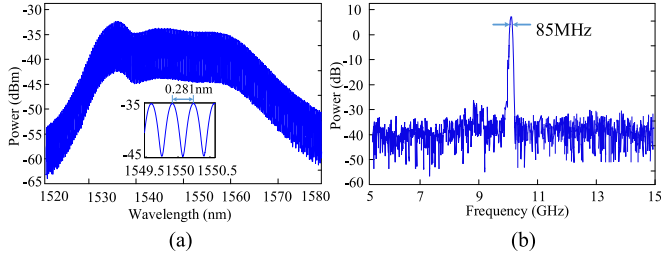


Fig. 11. (a) Optical spectrum measured at the output of the MZI. Inset: zoom-in view of the sliced spectrum. (b) Measured frequency response of the single passband MPF [7].

For temperature sensing, assuming that the length of the sensing arm that is subjected to a temperature perturbation  $L_1$ , the FSR of the MZI is given by

$$\begin{aligned} \Delta\lambda_{\text{FSR}}^1 &= \frac{\lambda^2}{n\Delta L_0 + \Delta n L_1 + n\Delta L_1} \\ &= \frac{\lambda^2}{n\Delta L_0 + n \cdot \xi \cdot \Delta T \cdot L_1 + n \cdot \alpha \cdot \Delta T \cdot L_1} \\ &= \frac{\lambda^2}{n\Delta L_0 + (\xi + \alpha) \cdot \Delta T \cdot n \cdot L_1} \end{aligned} \quad (2)$$

where  $\alpha$  ( $\sim 0.55 \times 10^{-6}/^\circ\text{C}$ ) is the thermal expansion coefficient of silica and  $\xi$  ( $\sim 6.45 \times 10^{-6}/^\circ\text{C}$ ) is the thermo-optic coefficient representing the temperature dependence of the refractive index of the fiber. The relationship between the frequency change and the applied temperature can be expressed as

$$\begin{aligned} \Delta f &= \frac{1}{D\Delta\lambda_{\text{FSR}}^1} - \frac{1}{D\Delta\lambda_{\text{FSR}}^0} \\ &= \frac{1}{D\lambda^2}(\eta + \alpha) \cdot \Delta T \cdot n \cdot L_1 \end{aligned} \quad (3)$$

As can be seen the microwave frequency change is linearly proportional to the temperature change. Thus, by measuring the frequency change, the temperature change can be estimated.

The operation of the OEO sensor was demonstrated. In the experiment, an ASE source with a spectral width of 30 nm was used which was sent to the MZI with an original length difference between the two arms of 4 mm. The spectrum is sliced by the MZI into more than 100 channels and the channel spacing or the FSR is 0.281 nm, as shown in Fig. 11(a). The sliced light wave was then sent to the MZM, where it is modulated by a microwave signal. The modulated light wave is sent to the DCF with a value of dispersion of 339 ps/nm. After passing through the DCF and amplified by the EDFA, the optical signal was converted to a microwave signal and amplified by the EA. The spectral response of the microwave photonic filter was measured without closing the OEO loop, which was done by using an ESA. Fig. 11(b) shows the measured frequency response of the microwave photonic filter. As can be seen a microwave filter with a single passband was realized. The 3-dB bandwidth of the frequency resonance is 85 MHz, which is sufficiently narrow to ensure a single-frequency oscillation of the OEO.

When the loop was closed, and the gains of the EA and the EDFA were controlled to make the total gain sufficiently high to compensate for the overall loop loss, microwave oscillation

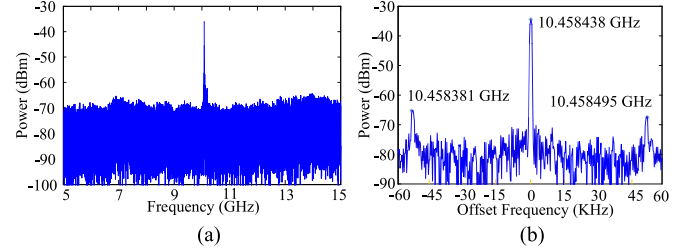


Fig. 12. (a) Electrical spectrum of the generated 10.458 GHz microwave signal at room temperature, here the resolution bandwidth (RBW) is 1.5 MHz. (b) Zoom-in view of the signal (the RBW is 1 KHz) [7].

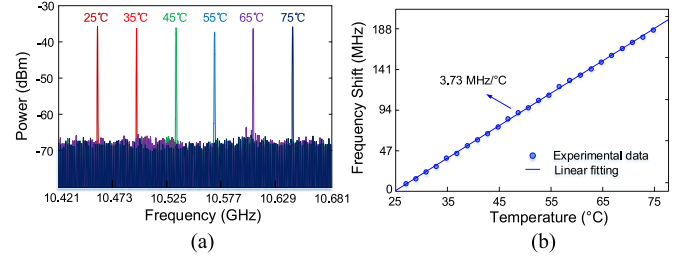


Fig. 13. (a) Superimposed electrical spectra of the generated microwave signal at different temperatures. (b) Measured oscillation frequency shift as a function of the applied temperature to the sensing arm from 25 °C to 75 °C with a step of 2 °C [7].

would start. Fig. 12(a) shows the spectrum of the generated microwave signal at 10.458 GHz measured at a room temperature, with a zoom-in view shown in Fig. 12(b). Side modes were observed. The first side mode is located at an offset frequency of 57 kHz, which indicates the FSR of the OEO loop is 57 kHz corresponding to a length of 3.6 km for the entire OEO loop. Since the main oscillation mode has a much higher power than the side modes, the frequency of the main oscillation mode can be correctly measured.

In the experiment, when the temperature applied to the sensing arm was increased from 25°C to 70°C, a microwave signal with its frequency changing from 10.458 GHz to 10.643 GHz was resulted. Fig. 13(a) shows the measured frequency shift as a function of the applied temperature. The sensitivity by linearly fitting the measured data in Fig. 13(b) was calculated to be 3.73 MHz/°C, which was much higher than that using a similar temperature sensor based on an OEO [13]. The reasons of having such a high sensitivity is because a small section of optical fiber was employed in the MZI, while in [13] the sensing element was the entire OEO loop. Thus, the relative length change was much smaller than fiber section used in the MZI.

## V. AN OEO SENSOR USING AN OEO-COUPLED DUAL-WAVELENGTH LASER

Another solution to avoid wavelength-drift-induced interrogation errors is to use an OEO incorporating an OEO-coupled dual-wavelength laser, instead of an independent laser source provided externally.

Fig. 14 shows the schematic of an OEO incorporating an OEO-coupled dual-wavelength laser [8]. It has two mutually coupled loops: the fiber ring loop and the OEO loop. In the fiber ring loop, a PM-PS-FBG is incorporated to generate two optical

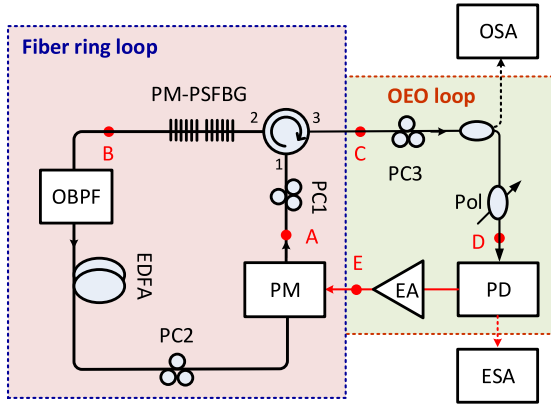


Fig. 14. The schematic of an OEO sensor incorporating an OEO-coupled dual-wavelength fiber ring laser [8]. PM: phase modulator; PC: polarization controller; PD: photodetector; EA: electrical amplifier; PM-PS-FBG: polarization maintaining phase-shifted fiber Bragg grating; OBPF: optical bandpass filter; Pol: polarizer; OSA: optical spectrum analyzer; ESA: electrical spectrum analyzer; EDFA: erbium-doped fiber amplifier.

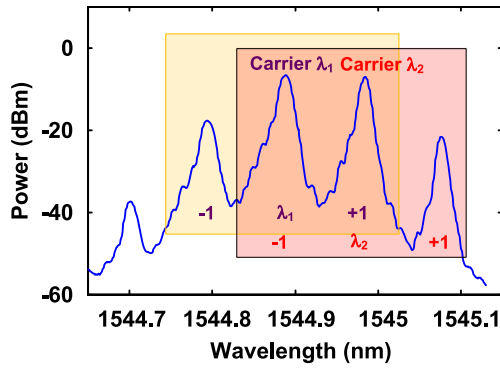


Fig. 15. The optical spectrum at the output of the fiber ring laser. Two wavelength are observed [8].

wavelengths  $\lambda_1$  and  $\lambda_2$  with the wavelength spacing determined by two ultra-narrow transmission bands due to the birefringence of the PM fiber in which the PM-PS-FBG is inscribed. In the OEO loop, a microwave signal with its frequency also determined by the birefringence of the PM fiber is generated, which is fed into the fiber ring loop to injection lock the dual wavelengths. The stable operation of the dual wavelengths is ensured due to the mutual injection locking. For example, for the wavelength at  $\lambda_1$ , the phase modulated signal has a sideband that is exactly located at the other transmission band of the PM-PS-FBG at  $\lambda_2$ , thus the sideband at  $\lambda_2$  will be injected into the fiber ring laser. Such injection provides extra energy to  $\lambda_2$ , which helps initialize and stabilize the lasing. The two wavelengths will finally reach a steady state, due to the nonlinear effect in the PM, in which the electric field at any point of the ring loop after a round trip should keep constant.

A very stable dual-wavelength operation is established due to the injection locking. The use of the OEO for high-resolution and high-speed transverse load sensing was implemented. Fig. 15 shows the spectrum of the dual wavelengths from the ring laser. Each wavelength serving as an optical carrier to generate a double-sideband with carrier (DSB + C) signal. Note that the DSB+C signal for the optical carrier at  $\lambda_1$  has its +1st

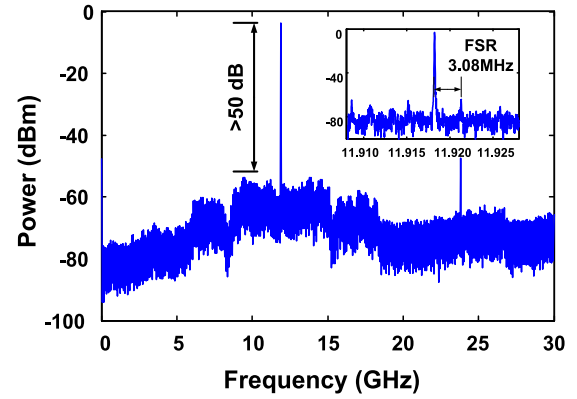


Fig. 16. The electrical spectrum of the microwave signal at the output of the PD [8].

order sideband located at the optical carrier at  $\lambda_2$ , and the DSB + C signal for the optical carrier at  $\lambda_2$  has its -1st order sideband located at the optical carrier at  $\lambda_1$ . This is the mutual coupling, which is the key mechanism that ensures a stable operation of the dual-wavelength fiber ring laser. Thanks to this mechanism, the injection would reduce the effect of mode competition and stabilize the dual-wavelength lasing.

When the dual wavelengths are fed into the OEO, a microwave signal is generated by the OEO. Since the oscillating frequency is only determined by the birefringence of the PM-PS-FBG, the frequency of the microwave signal is independent of the wavelengths of the optical carriers from the fiber ring laser. Thus, the wavelength drift will not affect the interrogation accuracy. By beating the two lasing wavelengths at the PD, a microwave signal is generated. Note that the frequency is determined by the intrinsic birefringence of the PM fiber and is not affected by the wavelength drift of the fiber ring laser. Fig. 16 shows the spectrum of the generated microwave signal. The signal power can reach -3 dBm with a SNR over 50 dB. A zoom-in view of the spectrum is shown as an inset in Fig. 16, which confirms the single-mode oscillation with a sidemode suppression ratio better than 50 dB. The FSR was measured to be 3.08 MHz, which is consistent with the total length OEO loop of about 60 m. A second peak at 23.6 GHz was observed, which was the 2nd harmonic generated due to nonlinearity of the OEO loop.

The use of the OEO for the measurement of a transverse load was performed, in which a transverse load was applied to the PM-PS-FBG. Again, to ensure the sensor to reach its highest sensitivity, the transverse load was applied to the PM-PS-FBG along its fast or slow axis. A supporting fiber with an identical radius was also placed in parallel with the PM-PS-FBG to guarantee that the load was applied to the PM-PS-FBG transversely, while sharing half of the applied load, as shown in Fig. 17(a). By increasing the load applied to the PM-PS-FBG, the beat frequency was shifted towards a higher frequency, as shown in Fig. 17(b), from 11.9033 to 12.3897 GHz, with a transverse load from 0 to 0.03969 N/mm.

According the theoretical analysis in [8], the frequency of the beat note is linearly proportional to the load applied to the fiber with a given angle between the force direction and the principal axis. The microwave frequency with the force applied along

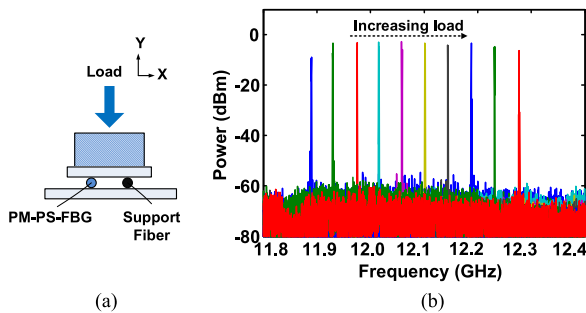


Fig. 17. (a) Setup for applying a transverse load to the PM-PS-FBG. (b) The electrical spectrum of the microwave signal with increasing the load applied to the PM-PS-FBG along the fast axis [8].

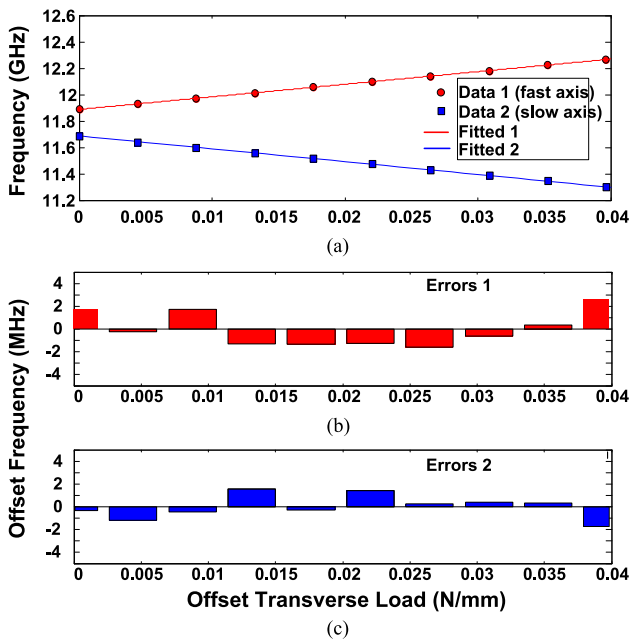


Fig. 18. (a) The measured microwave frequencies versus the transverse load along the fast axis (data1) and slow axis (data 2). (b) The errors between the measured frequencies and the linearly fitted curve along the fast axis of the PM-PS-FBG; (c) the errors between the measured frequencies and the linearly fitted curve along the slow axis of the PM-PS-FBG [8].

either the slow or the fast axis of the PM-PS-FBG was measured. First, a force along the slow axis of the PM-PS-FBG was applied. By increasing the force with a constant force increment of 0.00441 N/mm, the frequencies were measured and shown in Fig. 18(a) as solid squares. A linearly fitted curve was also shown. Then, a force along the fast axis of the PM-PS-FBG was applied. Again, the force was increased with a constant force increment of 0.00441 N/mm. The frequencies were measured and shown in Fig. 18(a) as solid circles. The frequency separation at a zero load was caused by an initial load applied to the PM-PSF-BG. By using the typical values of a silica fiber at a wavelength of 1550 nm:  $n_0 = 1.467$ ,  $p_{11} = 0.12$ ,  $p_{12} = 0.27$ ,  $\nu_p = 0.17$ ,  $E = 7.6 \times 10^4 \text{ N/mm}^2$  and the radius of optical fiber  $r = 62.5 \mu\text{m}$ , the theoretical sensitivity of the sensor was calculated to be 9.9 GHz/(N/mm), while the linearly fitted slopes

were 9.7573 GHz/(N/mm) and  $-9.7350 \text{ GHz}/(\text{N/mm})$  for the force applied along the fast and the slow axes, respectively. A good agreement between the theoretical and the experimental results was reached. The errors between the measured frequencies and the linearly fitted values, shown in Fig. 18(b) and (c), are all smaller than 3.08 MHz, which was within one FSR of the OEO loop. This illustrates that the microwave signal will oscillates at the discrete frequencies determined by the FSR which is close to the theoretical value where only the birefringence was taken into consideration. Therefore, the resolution of the system is determined by the FSR of the OEO loop. The resolution of the system was calculated as  $3.1566 \times 10^{-4} \text{ N/mm}$  or  $3.1638 \times 10^{-4} \text{ N/mm}$ , corresponding the FSR of 3.08 MHz, for a force applied along, respectively, the fast and slow axes in the experiment.

The measurement range of the optical probe can reach 7.5 N/mm which was determined by the spectral width from the ultra-narrow notch to one edge of its reflection band, which was about 75 GHz. The measurement range was also limited by the bandwidths of the components including the PD, the PM and the EA used in the experiment. Note that the measurement range was  $\sim 0.6 \text{ N/mm}$ , which was limited by the bandwidth of the EA (6-18 GHz) and the initial-birefringence-induced offset frequency (11.8 GHz) of the PM-PS-FBG.

## VI. CONCLUSION

OEO-based optical sensors for strain, temperature or transverse load sensing have been discussed. It is different from an OEO for microwave signal generation where the frequency selection element in an OEO can be a purely electronic microwave filter with a fixed center frequency, in an OEO-based optical sensor the frequency selection element should have a center frequency that is a function of the applied strain, temperature or transverse load. This was done by using a microwave photonic filter implemented by using either a PS-FBG to perform phase-modulation to intensity-modulation conversion by filtering out one first-order sideband of a phase-modulated optical signal, or a broadband light source sliced by an MZI, to produce a single-passband photonic microwave filter. By changing the strain, temperature or transverse load applied to the PS-FBG or the fiber in one arm of the MZI, the center frequency of the microwave photonic filter was changed. By incorporating the microwave photonic filter into an OEO, the oscillation frequency was also changed. The key advantage of an OEO-based optical sensor is its ultra-high resolution, since the optical wavelength measurement was translated to the microwave frequency measurement, which could be done using a DSP. In addition, the measurement speed is also much higher than an optical sensor using an OSA.

In addition to strain, temperature or transverse load measurement, an OEO based sensor can also be used as a biosensor for the diagnosis of diseases and environmental detection of biological agents. For example, an OEO-based optical sensor can be used for refractive index measurement thanks to its ultra-high sensitivity and resolution. In this case, an optical fiber with its cladding removed and replaced by gold coating in the sensing region to produce the plasmon resonance, which is identified by a



dip in the transmission spectrum of the guided optical wave [14]. A tilted fiber Bragg grating assisted surface plasmon resonance would have a narrower dip [15]. If the dip is narrow enough, the gold-coded fiber can be used to replace the PS-FBG to perform a microwave photonic filter for refractive index sensing.

## REFERENCES

- [1] A. Neyer and E. Voges, "Hybrid electro-optical multivibrator operating by finite feedback delay," *Electron. Lett.*, vol. 18, no. 2, pp. 59–60, Jan. 1982.
- [2] X. S. Yao and L. Maleki, "Optoelectronic microwave oscillator," *J. Opt. Soc. Amer. B*, vol. 13, no. 8, pp. 1725–1735, Aug. 1996.
- [3] J. P. Yao, "Microwave photonics for high resolution and high speed interrogation of fiber Bragg grating sensors," *Fiber Integrated Opt.*, vol. 34, no. 4, pp. 230–242, Oct. 2015.
- [4] M. Li, W. Li, J. P. Yao, and J. Azana, "Femtometer-resolution wavelength interrogation using an optoelectronic oscillator," presented at the IEEE Photon. Conf., Burlingame, CA, USA, Sep. 23–27, 2012.
- [5] W. Li, M. Li, and J. P. Yao, "A narrow-passband and frequency-tunable micro-wave photonic filter based on phase-modulation to intensity-modulation conversion using a phase-shifted fiber Bragg grating," *IEEE Trans. Microw. Theory Techn.*, vol. 60, no. 5, pp. 1287–1296, May 2012.
- [6] F. Kong, W. Li, and J. P. Yao, "Transverse load sensing based on a dual-frequency optoelectronic oscillator," *Opt. Lett.*, vol. 38, no. 14, pp. 2611–2613, Jul. 2013.
- [7] Y. Wang, J. Zhang, and J. P. Yao, "An optoelectronic oscillator for high sensitivity temperature sensing," *IEEE Photon. Technol. Lett.*, vol. 28, no. 13, pp. 1458–1461, Jul. 2016.
- [8] F. Kong, B. Romeira, J. Zhang, W. Li, and J. P. Yao, "A dual-wavelength fiber ring laser incorporating an injection-coupled optoelectronic oscillator and its application to transverse load sensing," *J. Lightw. Technol.*, vol. 32, no. 9, pp. 1784–1793, May 2014.
- [9] S. M. Melle, K. Liu, and R. M. Measures, "A passive wavelength demodulation system for guided-wave Bragg grating sensors," *IEEE Photon. Technol. Lett.*, vol. 4, no. 5, pp. 516–518, May 1992.
- [10] M. Song, S. Yin, and P. B. Ruffin, "Fiber Bragg grating strain sensor demodulation with quadrature sampling of a Mach-Zehnder interferometer," *Appl. Opt.*, vol. 39, no. 7, pp. 1106–1111, Jul. 2000.
- [11] M. Li, W. Li, and J. P. Yao, "Tunable optoelectronic oscillator incorporating a high-Q spectrum-sliced photonic microwave transversal filter," *IEEE Photon. Technol. Lett.*, vol. 24, no. 14, pp. 1251–1253, Jul. 2012.
- [12] J. Zhang, L. Gao, and J. P. Yao, "Tunable optoelectronic oscillator incorporating a single passband microwave photonic filter," *IEEE Photon. Technol. Lett.*, vol. 26, no. 4, pp. 326–329, Feb. 2014.
- [13] Y. Zhu, X. Jin, H. Chi, S. Zheng, and X. Zhang, "High-sensitivity temperature sensor based on an optoelectronic oscillator," *Appl. Opt.*, vol. 53, no. 22, pp. 5084–5087, Aug. 2014.
- [14] R. C. Jorgenson and S. S. Yee, "A fiber-optic chemical sensor based on surface plasmon resonance," *Sens. Actuators B Chem.*, vol. 12, no. 3, pp. 213–220, 1993.
- [15] C. Caucheteur, T. Guo, and J. Albert, "Review of plasmonic fiber optic biochemical sensors: improving the limit of detection," *Anal. Bioanal. Chem.*, vol. 407, no. 15, pp. 3883–3897, May 2015.

**Jianping Yao** (M'99–SM'01–F'12) received the Ph.D. degree in electrical engineering from the Université de Toulon et du Var, France, in December 1997. He is a Professor and the University Research Chair in the School of Electrical Engineering and Computer Science, University of Ottawa, Ottawa, ON, Canada. From 1998 to 2001, he was with the School of Electrical and Electronic Engineering, Nanyang Technological University, Singapore, as an Assistant Professor. In December 2001, he joined the School of Electrical Engineering and Computer Science, University of Ottawa, as an Assistant Professor, where he became an Associate Professor in 2003, and a Full Professor in 2006. He was appointed the University Research Chair in Microwave Photonics in 2007. In 2016, he received the title of Distinguished University Professor at the University of Ottawa. From July 2007 to June 2010 and July 2013 to June 2016, he was the Director of the Ottawa–Carleton Institute for Electrical and Computer Engineering.

He has authored or co-authored more than 510 research papers, including more than 300 papers in peer-reviewed journals and 210 papers in conference proceedings. He is a Topical Editor for *Optics Letters*, and serves on the Editorial Boards of the IEEE TRANSACTIONS ON MICROWAVE THEORY AND TECHNIQUES, *Optics Communications*, the *Frontiers of Optoelectronics*, and *Science Bulletin*. He was a Guest Co-Editor for a Focus Issue on Microwave Photonics in *Optics Express* in 2013 and a Lead Editor for a Feature Issue on Microwave Photonics in *Photonics Research* in 2014. He is the Chair of numerous international conferences, symposia, and workshops, including the Vice Technical Program Committee (TPC) Chair of the IEEE Microwave Photonics Conference in 2007, the TPC Co-Chair of the Asia-Pacific Microwave Photonics Conference in 2009 and 2010, the TPC Chair of the high-speed and broadband wireless technologies subcommittee of the IEEE Radio Wireless Symposium in 2009–2012, the TPC Chair of the microwave photonics subcommittee of the IEEE Photonics Society Annual Meeting in 2009, the TPC Chair of the IEEE Microwave Photonics Conference in 2010, the General Co-Chair of the IEEE Microwave Photonics Conference in 2011, the TPC Co-Chair of the IEEE Microwave Photonics Conference in 2014, and the General Co-Chair of the IEEE Microwave Photonics Conference in 2015. He is also a committee member of numerous international conferences, such as IPC, OFC, BGPP, and MWP. He received the 2005 International Creative Research Award from the University of Ottawa. He received the 2007 George S. Glinski Award for Excellence in Research. In 2008, he received Natural Sciences and Engineering Research Council of Canada Discovery Accelerator Supplements Award. He was selected to receive an inaugural OSA Outstanding Reviewer Award in 2012. He was an IEEE MTT-S Distinguished Microwave Lecturer for 2013–2015.

Prof. Yao is a registered Professional Engineer of Ontario. He is a Fellow of the Optical Society of America and the Canadian Academy of Engineering.